Indonesian Journal of Electrical Engineering and Computer Science
Vol. 27, No. 3, September 2022, pp. 1290~1296
ISSN: 2502-4752, DOI: 10.11591/ijeecs.v27.i3.pp1290-1296

$Ca_9La(PO_4)_7:Eu^{2+},Mn^{2+}$: a radiation-adjustable phosphor usable for high-perfomance white light-emitting diodes

Phuc Dang Huu[1], Phung Ton That[2], Phan Xuan Le[3], Nguyen Le Thai[4]
[1]Faculty of Fundamental Science, Industrial University of Ho Chi Minh City, Ho Chi Minh City, Vietnam
[2]Faculty of Electronics Technology, Industrial University of Ho Chi Minh City, Ho Chi Minh City, Vietnam
[3]Faculty of Mechanical-Electrical and Computer Engineering, School of Engineering and Technology, Van Lang University, Ho Chi Minh City, Vietnam
[4]Faculty of Engineering and Technology, Nguyen Tat Thanh University, Ho Chi Minh City, Vietnam

Article Info

Article history:

Received Nov 29, 2021
Revised Jun 4, 2022
Accepted Jun 25, 2022

Keywords:

$Ca_9La(PO_4)_7:Eu^{2+},Mn^{2+}$
Color homogeneity
Luminous flux
Monte Carlo theory
White light-emitting diodes

ABSTRACT

We used solid-condition processes to make a sequence of radiation-adjustable phosphors Eu^{2+}/Mn^{2+} co-doped $Ca_9La(PO_4)_7$ (shortened as CaLa:EM), which show a consistently variable hue from green to yellow and red via an efficient resonance-form energy transition as well as the strength of green and red radiations may be controllable through altering the Mn^{2+} concentration. We examined the transition of energy ($Eu^{2+} \rightarrow Mn^{2+}$) for CaLa:EM. It is proved to be a resonant kind using a dipole-quadrupole process, having power shift critical range calculated to be 11.36 Å by using the spectral overlap techniques. Mixing a 365 nm UV-InGaN chip as well as one phosphor combination containing $(Ca_{0.98}Eu_{0.005}Mn_{0.015})_9La(PO_4)_7$ in yellow with $BaMgAl_{10}O_{17}:Eu^{2+}$ in blue produced a warming WLED having CIE color coordinates measured at (0.35, 0.31), better CRI value (*Ra*) measured at 91.5 along with smaller CCT value of 4,496 K.

Corresponding Author:

Phan Xuan Le
Faculty of Mechanical-Electrical and Computer Engineering, School of Engineering and Technology
Van Lang University
Ho Chi Minh City, Vietnam
Email: le.px@vlu.edu.vn

1. INTRODUCTION

White light-emitting diodes (WLEDs) have received a lot of attention in recent times. It is possible to create white lighting through one InGaN chip in blue as well as a phosphor $Y_3Al_5O_{12}:Ce^{3+}$ garnet ($YAG:Ce^{3+}$) in yellow. Even so, because of the shortage of red spectral contribution, this technique has an inferior CRI (*Ra* value of 75) as well as an elevated hue temperature (CCT = 7,756 K) [1], [2]. White LEDs manufactured utilize (a) non-ultraviolet or ultraviolet LED (350,420 nm) as well as red, green, as well as blue phosphors [3], [4], (b) non-ultraviolet LED (380,420 nm) pumped with one singular structure green-to-red radiation-adjustable [5], [6] and blue phosphor to enhance the CRI as well as CCT. In such a situation, single-component yellow-light phosphors, which include green Eu^{2+} along with red Mn^{2+}, used to create UV or n-UV excitations have piqued the interest of solid-state lighting researchers. In comparison with the blue LED chip (made of InGaN) and the phosphor $YAG:Ce^{3+}$, a white-light diode manufactured utilizing the combination which includes single-component radiation-adjustable phosphor along with blue phosphor pumped with non-ultraviolet (or ultraviolet) chips has a higher CRI, adjustable CCT along with CIE color coordinates. A method used to produce one-phase radiation-adjustable phosphor involves co-doping the similar host with the sensitizer as well as the activator. The host relies on the nature of the power transmission between the sensitizer and the activator. The phosphors possessing sensitizer/activator power transmission mechanisms, including Eu^{2+}/Mn^{2+}, were produced as well as studied for a variety of hosts. To the best of our understanding, no one has mentioned the crystal structure, brightness characteristics, or transmission of energy for Eu^{2+}/Mn^{2+} of $Ca_9La(PO_4)_7$. We first illustrated a one-component green-to-red radiation-adjustable CaLa:EM that is adjustable between green, yellow and red via transmission of energy mechanism among the illumination centers Eu^{2+} and Mn^{2+}. We have shown that raising the dopant content of Mn^{2+} can result in warm white lighting as well. CaLa:EM has the wonderful promise of usage in the form of a one-stage phosphor pumpable using near-ultraviolet or ultraviolet LED devices in white UV-LED implementations [7], [8].

2. EXPERIMENTAL

2.1. Preparation of green-emitting CaLa:EM phosphor

Powder X-ray diffraction (XRD), photoluminescence (PL) as well as PL excitation (PLE) spectra, decay duration, along with CIE chromatic features were used to typify the samples, as noted in the earlier work [6], [7]. We compressed the testing portions of powder and subjected them to excitation at an incidence angle of 45°. To have the green-phosphor CaLa:EM, its essential chemical components and creation process are presented in Table 1. Particularly, the composition of CaLa:EM includes $CaCO_3$, Y_2O_3, La_2O_3, $(NH_4)_2HPO_4$, Eu_2O_3, and MnO with the purity of ≥99%. Next, Table 2 details the instruments for determining the characteristics of attained CaLa:EM phosphor including phase purity, photoluminescence (PL) spectra, released fluorescence, time-resolved measurements, and radiation transients.

Table 1. The components and process of creating CaLa:EM

Components	Purity	Process
$CaCO_3$	99.9%	- Compress the components into pellets
Y_2O_3	99.99%	
La_2O_3	99%	- Calcinate the substances for eight hours under 1,473K within an ambient atmosphere
$(NH_4)_2HPO_4$	99%	
Eu_2O_3	99.99%	- Substances are processed under 1,273K within eight hours in an alumina boat below a
MnO	99.9%	lowering atmosphere of 15% H_2/85% N_2

Table 2. Assessing the characteristics of CaLa:EM

Characteristics	Determining tools
Phase purity	Powder XRD assessment accompanied by Bruker AXS D8 advanced automatic diffractometer as well as Cu Kα radiation
PL, PLE spectra	Spex Fluorolog-3 Spectrofluorometer (Instruments SA, N.J., USA) accompanied by one Xe light under 450 watts as well as dual stimulation monochromators
Released fluorescence	Photomultiplier of the form Hamamatsu Photonics R928 at 90^0 angle to the stimulation ray
Time-resolved measurements	Adjustable nanosecond optical-parametric-oscillator/Q-switch-pumped YAG:Nd^{3+} laser formation (NT341/1/UV, Ekspla)
Radiation transients	Obtained using nanochromater (ARC's SpectraPro300i), detected using a photomultiplier tube (R928HA, Hamamatsu), linked to a digital oscilloscope (LT372, LeCrop) as well as transmitted towards a computer to study kinetics [9], [10]

We created WLED lightings via combining clear silicon resin with phosphor mixture of CaLa:EM along with $BaMgAl_{10}O_{17}:Eu^{2+}$ above an ultraviolet chip (AOT Product No: DC0004CAA, Spec: 370U02C, maximum wavelength: 365 ~370 ± 0.6 nm, chip size: 40x40 mil, forward voltage: 3.8 ~4.0 ± 0.02 V, power: 10-20 ± 0.21 mW). All samples had their chromaticity coordinates evaluated by the Commission International de I'Eclairage (CIE). The phosphor film in the actual MCW-LED is reproduced using flat silicone films and the LightTools 9.0 application, and the Monte Carlo method [11]-[14]. This simulated method works throughout the following phases: (1) Establish and build the layout as well as optical features of MCW-LED lamps (2). The CaLa:EM concentration variation then controls the optical impacts of the phosphor combining. For the task of assessing the influence of YAG:Ce^{3+} as well as CaLa:EM imposed on MCW-LED device, we made several collations. It is specified that the two kinds of two-sheet distant phosphors, under 3000 K and 5000 K, need to be defined. Figure 1 illustrates an MCW-LED device containing conformal phosphor under one median CCT measured at 8500 K. Recreating MCW-LED devices with constituents other than CaLa:EM is also considered. The reflector's bottom length, height, and length of the top surface are determined as follows: 8 mm, 2.07 mm, and 9.85 mm. The conformal phosphor combining surrounds 0.08-mm-thick nine chips. Every chip stays on the cavity of the reflector via a square base zone measured at 1.14 mm2 along with a height measured at 0.15 mm. The luminous flux in all chips reaches 1.16 W, with a maximum wavelength reaching 453 nm [15]-[17].

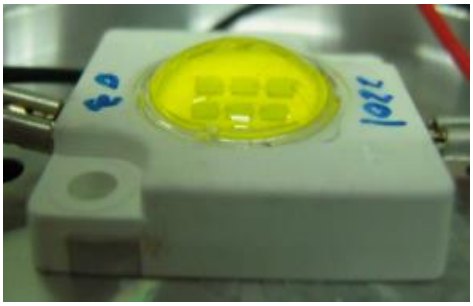

Figure 1. A WLED device

2.2. Characterization of phosphor

To analyze the transiting energy of the electrons within CaLa:EM phosphor geometry, the crystal field splitting is accessed. Crystal field splitting (*Dq*) will be demonstrated via the following expression [18]. Additionally, in (1), the *Dq* is carried out through Königs *et al.* [19] as well as Tsai *et al.* [20].

$$D_q = \frac{1}{6} Z e^2 \frac{r^4}{R^5} \tag{1}$$

Where *Dq* is a power level separation assessment. *Z* indicates an anion charge. *e* indicates an electron charge. *r* indicates the radius for the *d* wave function. *R* indicates the binding range. With the Y^{3+} site replaced, then taken via a bigger La^{3+} ion, the range among Eu^{2+} as well as O^{2-} was reduced. Because crystal field splitting correlates with $1/R^5$, the smaller Eu^{2+} O^{2-} length raises the crystal field's size, yielding a penalty for the 5*d* line in Eu^{2+}. In (2) [21], [22] best fits the corresponding brightness decay periods with a second-order exponential decay mode:

$$I = A_1 \exp(-t/\tau_1) + A_2 \exp(-t/\tau_2) \tag{2}$$

in the (3), *I* represents the brightness strength; A_1, along with A_2, represents constants, *t* represents time; τ_1 and τ_2 correspondingly represent the quick and sluggish lifetimes of exponential elements. Utilizing such factors, it is possible to calculate the mean decay periods (τ) by utilizing a (3) [11].

$$\langle \tau \rangle = (A_1\tau_1^{\,2} + A_2\tau_2^{\,2}) / (A_1\tau_1 + A_2\tau_2) \tag{3}$$

The attained and evaluated τ_1, τ_2, A_1, and A_2 indicate that the mean decay period in a solely Eu^{2+}-activated system is long. The mean decay period was noticed to be reduced with raising doped Mn^{2+} content in the Eu^{2+}/Mn^{2+} co-doped formation.

3. RESULTS AND ANALYSIS

Figure 2 depicts the inverse change in concentration of green phosphorus CaLa:EM and phosphorus YAG:Ce^{3+} in yellow. The transformation signifies the following: maintaining high CCT values and affecting the absorption as well as the dispersion in WLEDs with the dual layers of phosphor. This eventually influences the hue output as well as the lighting beam effectiveness in the WLED devices. Thus, the CaLa:EM concentration chosen determines the hue quality of WLEDs. When the CaLa:EM concentration increased (2%-20%) by weight, the YAG:Ce^{3+} content decreased for the purpose of retaining the mean CCTs, which is true for the 3000 K and 5000 K WLEDs, see Figures 2(a) and 2(b), respectively.

Figure 3 illustrates the effect of CaLa:EM green phosphorus concentration on the emissivity spectrum in the WLED device. It is probable to have a selection by judging the demands of the producers. WLED devices demanding significant hue quality can decrease lighting flux by a small portion. As seen in Figure 3, the area of the spectrum generates white illumination. The spectrum of 3000 K is shown in Figure 3(a) while that of 5000 K is illustrated in Figure 3(b). The intensity surges alongside the CaLa:EM content of two areas in the light spectrum: 420-480 nm as well as 500-640 nm. Such transformation within the radiation spectrum with two bands shows a greater illuminating beam. Furthermore, blue-light dispersion in WLED is increased, implying that dispersion within the sheet of phosphor as well as WLED device would be risen, preferring hue homogeneity. This is a significant result when we empoly CaLa:EM. Controlling the hue homogeneity for the distant phosphor layout under huge temperature, in specific, proves challenging. This results proved that CaLa:EM, under color temperatures (5600 K as well as 8500 K), can result in superior hue output in WLED devices.

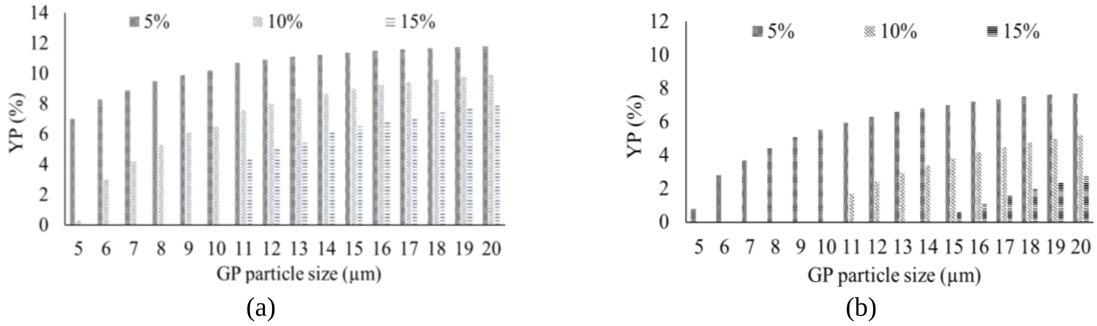

Figure 2. Modifying phosphor content for the task of retaining the mean CCT at (a) 3000 K and (b) 5000 K

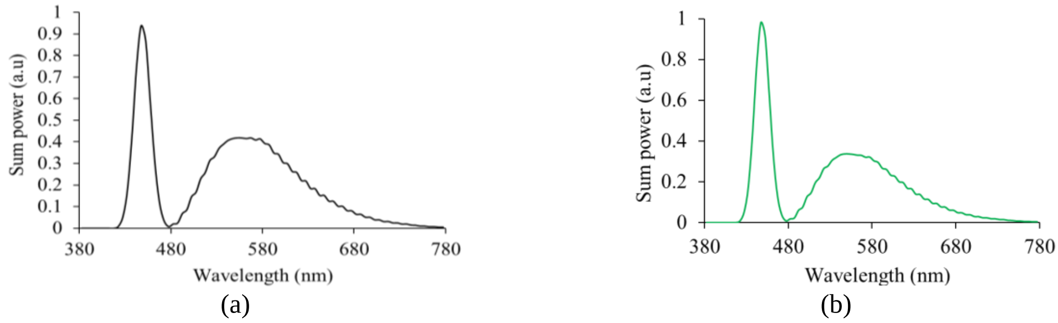

Figure 3. Radiation spectra along with CaLa:EM content for (a) 3000 K and (b) 5000 K WLED devices

Accordingly, the increases in WLEDs' luminous intensities are improved with the increasing content of CaLa:EM phosphor, as shown in Figure 4. From the data in Figures 4(a) and (b), at both hue temperatures, the luminous fluxes of the WLEDs enhance when the weight percentage of the green phosphor increases to 10% and 15%. With such improvements in luminosity, hue quality must be carefully considered. The deviating color index (D-CCT) shown in Figure 5 is used to evaluate the homogeneity of the distributed color elements on the chroma scale. Specifically, Figure 5(a) shows the D-CCT at 3000 K, and Figure 5(b) shows the D-CCT at 5000 K. In both cases, the deviating color is reduced as the CaLa:EM phosphor weight percentages increase. This means the hue homogeneity of both WLEDs is improved with the increasing content of the CaLa:EM phosphor.

Hue homogeneity is the only element taken into account for examining the hue quality in WLED devices. The color standard is not guaranteed to be great with a high hue homogeneity index. As a result, previous findings show a color rendering index (CRI) and a color quality scale (CQS). As CRI is illuminated, the actual hue of an item is revealed. The hue imbalance is largely made up of green light between the vital hues: blue, yellow, and green, which alters the hue output of WLEDs, causing a reduction in WLED hue fidelity. The results in Figure 6 show a small decline in CRI in the existence of the distant phosphor CaLa:EM film, at both 3000 K (Figure 6(a)) and 5000 K (Figure 6(b)). On the other hand, such results can be acceptable since the color rendering index solely appears to be a drawback of CQS. Judging the CRI as well as the CQS, the latter appears to be of greater importance. It is also harder when it comes to achieving CQS. It is decided via the following facets: CRI, preference of beholder, as well as hue coordinate. Therefore, it becomes a precise overall index to determine hue quality [23]-[26]. Figure 7 shows the CQS improvement when the remote phosphor CaLa:EM film is present. Specifically, when using CaLa:EM with higher concentration, though the reduction in CQS is observed in the case of 3000 K WLED, it is insignificant, as shown in Figure 7(a). On the other hand, for the WLED with 5000 K, see Figure 7(b), when increasing the phosphor concentration of CaLa:EM to 10%, the CQS is unchanged. This means it is possible to attain good CQS when increasing the content of CaLa:EM for better luminosity. As the CaLa:EM content exceeds 10% wt., CRI and CQS will be drastically reduced owing to severe hue waste if green becomes dominating. Consequently, before utilizing CaLa:EM, determining suitable concentration would be important.

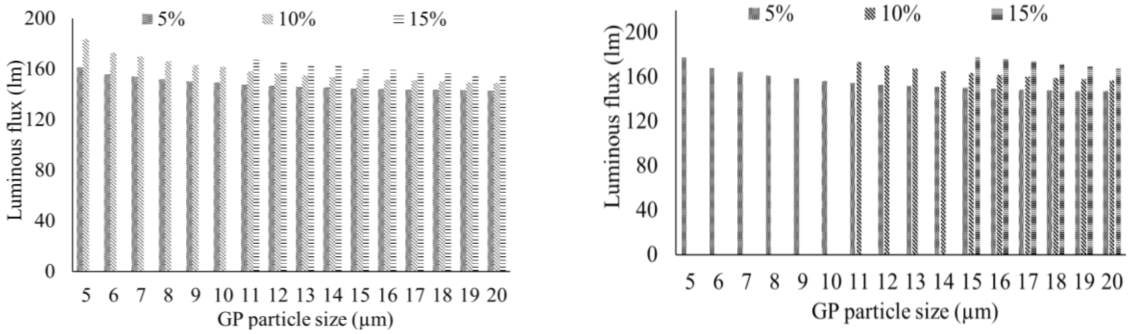

(a) (b)

Figure 4. The lighting beam in WLED device along with CaLa:EM content at (a) 3000 K and (b) 5000 K

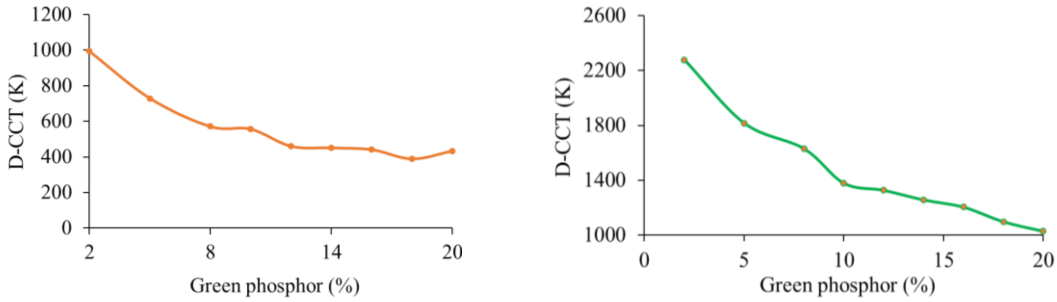

(a) (b)

Figure 5. The hue deviation in WLED device along with CaLa:EM content at (a) 3000 K and (b) 5000 K

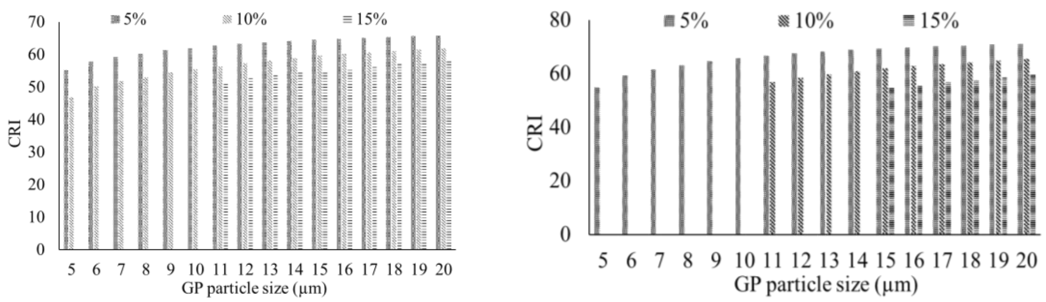

(a) (b)

Figure 6. The hue rendering index in WLED device along with CaLa:EM content at (a) 3000 K and (b) 5000 K

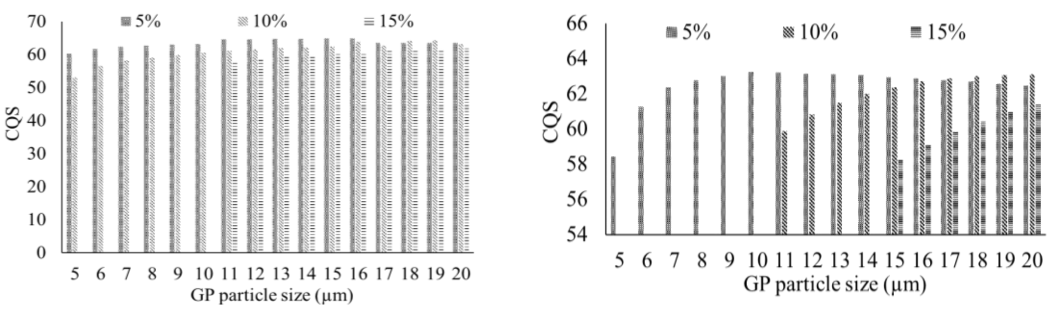

(a) (b)

Figure 7. The hue quality scale in WLED device along with CaLa:EM content at (a) 3000 K and (b) 5000 K

4. CONCLUSION

Finally, we created as well as inspected a sequence of radiation-adjustable CaLa:EM with single compositions. Furthermore, we studied as well as demonstrated the transferring energy ($Eu^{2+} \rightarrow Mn^{2+}$) of $Ca_9La(PO_4)_7$, which is resonant through a dipolequadrupole mechanism relying on the decay lifetime information, with the energy transmission critical spacing widely expected to be 11.36 Å through utilizing the spectrum overlay approach. By combining the yellow-light CaLa:EM with the blue-light $BaMgAl_{10}O_{17}$:Eu^{2+} pumped using an ultraviolet chip in LED, we enhanced the Ra as well as lowered the CCT in WLED devices (365 nm). Our findings show that ultraviolet-WLEDs relying on a mixture containing CaLa:EM, as well as BAM:Eu^{2+} outperform traditional WLED devices made of YAG:Ce^{3+} and blue LED chips in terms of *Ra* and CCT.

ACKNOWLEDGEMENTS

This study was financially supported by Van Lang University, Vietnam.

REFERENCES

[1] A. S. Praveen, R. Jithin, K. N. Kumar, and M. Baby, “Analysis of thermal and optical characteristics of light-emitting diode on various heat sinks,” *International Journal of Ambient Energy*, vol. 42, pp. 854-859, 2021, doi: 10.1080/01430750.2019.1567585.
[2] R. Srimathi and S. Hemamalini, “LED boost driver topologies for low voltage DC distribution systems in smart structured buildings,” *Electric Power Components and Systems,* vol. 46, pp. 1134-1146, 2018, doi: 10.1080/15325008.2018.1488301.
[3] C. N. Liao, H.-J. Chiu, and Y.-C. Hsieh, “Wide-range dimmable LED lighting based on QL-SEPIC converter,” *EPE Journal*, vol. 29, pp. 25-37, 2019, doi: 10.1080/09398368.2018.1494671.
[4] K. I. Hwu and Y.-T. Yau, “Series-based AC LED driver with efficiency improved,” *Electric Power Components and Systems*, vol. 46, pp. 637-646, 2018, doi: 10.1080/15325008.2018.1463579.
[5] A. P. García and A. Sędziwy, “Optimizing lighting of rural roads and protected areas with white light: a compromise among light pollution, energy savings, and visibility,” *LEUKOS*, vol. 16, pp. 147-156, 2020, doi: 10.1080/15502724.2019.1574138.
[6] H. Chen and S.-T. Wu, “Advanced liquid crystal displays with supreme image qualities,” *Liquid Crystals Today*, vol. 28, pp. 4-11, 2019, doi: 10.1080/1358314X.2019.1625138.
[7] M. P. Royer, K. W. Houser, and A. David, “Chroma shift and gamut shape: going beyond average color fidelity and gamut area,” *LEUKOS,* vol. 14, no. 3, pp. 149-165, 2018, doi: 10.1080/15502724.2017.1372203.
[8] M. O. Babatunde, T. O. Akinbulire, P. O. Oluseyi, and M. U. Emezirinwune, “Techno-economic viability of off-grid standalone PV-powered LED street lighting system in Lagos, Nigeria,” *African Journal of Science, Technology, Innovation and Development,* vol. 11, pp. 807-819, 2019, doi: 10.1080/20421338.2019.1586112.
[9] Q. Xue and G. Xie, “Easily reproducible top-emitting organic light-emitting devices for microdisplays adapted to aluminum contact from the standard CMOS processes,” *Journal of Information Display,* vol. 21, pp. 131-137, 2020, doi: 10.1080/15980316.2020.1773551.
[10] M. Hämmer, A. Gassmann, A. Reller, H. V. Seggern, O. Gutfleisch, R. Stauber, and J. Zimmermann, “Recyclable phosphor sheet based on polyvinyl alcohol for LED lighting using remote phosphor technology,” *Materials Technology,* vol. 34, pp. 178-183, 2019, doi: 10.1080/10667857.2018.1541213.
[11] Y. Jen *et al.*, "Design of an energy-efficient marine signal light based on white LEDs," *OSA Continuum*, vol. 2, pp. 2460-2469, 2019, doi: 10.1364/OSAC.2.002460.
[12] Y. Fang *et al.*, "Giant enhancement of white light emission from Ca9Ln(PO4)7:Eu2+,Mn2+ (Ln = La, Lu, Gd) phosphors achieved by remote aluminum reduction," *Opt. Mater. Express*, vol. 10, pp. 1306-1322, 2020, doi: 10.1364/OME.390069.
[13] Q. Guo *et al.*, "Characterization of YAG:Ce phosphor dosimeter by the co-precipitation method for radiotherapy," *Appl. Opt*, vol. 60, pp. 3044-3048, 2021, doi: 10.1364/AO.419800.
[14] H. Yuce, T. Guner, S. Balci, and M. M. Demir "Phosphor-based white LED by various glassy particles: control over luminous efficiency," *Opt. Lett*, vol. 44, pp. 479-482, 2019, doi: 10.1364/OL.44.000479.
[15] Z. Zhang, W. Li, N. Ma, and X. Huang, "High-brightness red-emitting double-perovskite phosphor Sr2LaTaO6:Eu3+ with high color purity and thermal stability [Invited]," *Chin. Opt. Lett*, vol. 19, pp. 030003, 2021, doi: 10.3788/COL202119.030003.
[16] D. Tuyet *et al.,* "Deep red fluoride dots-in-nanoparticles for high color quality micro white light-emitting diodes," *Opt. Express,* vol. 28, pp. 26189-26199, 2020, doi: 10.1364/OE.400848.
[17] S. Matsumoto and A. Ito "Chemical vapor deposition route to transparent thick films of Eu3+-doped HfO2 and Lu2O3 for luminescent phosphors," *Opt. Mater. Express,* vol. 10, pp. 899-906, 2020, doi: 10.1364/OME.386425.
[18] P. Ranjith, A. Manimaran, A. S. Praveen, and T. Ramesh, “Experimental investigation of heat transfer characteristics of the LED module using passive heat sinks,” *International Journal of Ambient Energy,* vol. 41, pp. 1209-1213, 2020, doi: 10.1080/01430750.2018.1507934.
[19] S. Königs, S. Mayr, and A. Buchner, “A common type of commercially available LED light source allows for colour discrimination performance at a level comparable to halogen lighting,” *Ergonomics,* vol. 62, pp. 1462-1473, 2019, doi: 10.1080/00140139.2019.1663940.
[20] B. K. Tsai, C. C. Cooksey, D. W. Allen, C. C. White, E. Byrd, and D. Jacobs, "Exposure study on UV-induced degradation of PTFE and ceramic optical diffusers," *Appl. Opt,* vol. 58, pp. 1215-1222, 2019, doi: 10.1364/AO.58.001215.
[21] N. C. A. Rashid *et al.,* "Spectrophotometer with enhanced sensitivity for uric acid detection," *Chin. Opt. Lett.,* vol. 17, p. 081701, 2019, doi: 10.3788/COL201917.081701.
[22] A. Ahmad, A. Kumar, V. Dubey, A. Butola, B. S. Ahluwalia, and D. S. Mehta, "Characterization of color cross-talk of CCD detectors and its influence in multispectral quantitative phase imaging," *Opt. Express,* vol. 27, pp. 4572-4589, 2019, doi: 10.1364/OE.27.004572.
[23] C. Tian *et al.*, "Mn4+ activated Al2O3 red-emitting ceramic phosphor with excellent thermal conductivity," *Opt. Express*, vol. 27, pp. 32666-32678, 2019, doi: 10.1364/OE.27.032666.

[24] R. Wan *et al.*, "Simultaneously improve the luminous efficiency and color-rendering index of GaN-based white-light-emitting diodes using metal localized surface plasmon resonance," *Opt. Lett*, vol. 44, pp. 4155-4158, 2019, doi: 10.1364/OL.44.004155.
[25] S. Abeysekera, V. Kalavally, M. Ooi, and Y. C. Kuang, "Impact of circadian tuning on the illuminance and color uniformity of a multichannel luminaire with spatially optimized LED placement," *Opt. Express*, vol. 28, pp. 130-145, 2020, doi: 10.1364/OE.381115.
[26] C. Wu *et al.*, "Phosphor-converted laser-diode-based white lighting module with high luminous flux and color rendering index," *Opt. Express*, vol. 28, pp. 19085-19096, 2020, doi: 10.1364/OE.393310.

BIOGRAPHIES OF AUTHORS

Phuc Dang Huu received a Physics Ph.D. degree from the University of Science, Ho Chi Minh City, in 2018. Currently, he is a lecturer at the Faculty of Fundamental Science, Industrial University of Ho Chi Minh City, Ho Chi Minh City, Vietnam. His research interests include simulation LEDs material, renewable energy. He can be contacted at email: danghuuphuc@iuh.edu.vn.

Phung Ton That was born in Thua Thien-Hue, Vietnam. He received the B.Sc. degree in electronics and telecommunications engineering (2007) and the M.Sc. degree in electronics engineering (2010) from the University of Technology, Vietnam. He is currently a lecturer at the Faculty of Electronics Technology (FET), Industrial University of Ho Chi Minh City. His research interests are optical materials, wireless communication in 5G, energy harvesting, performance of cognitive radio, physical layer security and NOMA. He can be contacted at email: tonthatphung@iuh.edu.vn.

Phan Xuan Le received a Ph.D. in Mechanical and Electrical Engineering from Kunming University of Science and Technology, Kunming city, Yunnan province, China. Currently, He is a lecturer at the Faculty of Engineering, Van Lang University, Ho Chi Minh City, Viet Nam. His research interests are Optoelectronics (LED), Power transmission and Automation equipment. He can be contacted at email: le.px@vlu.edu.vn.

Nguyen Le Thai received his BS in Electronic engineering from Danang University of Science and Technology, Vietnam, in 2003, MS in Electronic Engineering from Posts and Telecommunications Institute of Technology, Ho Chi Minh, Vietnam, in 2011 and PhD degree of Mechatronics Engineering from Kunming University of Science and Technology, China, in 2016. He is a currently with the Nguyen Tat Thanh University, Ho Chi Minh City, Vietnam. His research interests include the renewable energy, optimisation techniques, robust adaptive control and signal processing. He can be contacted at email: nlthai@nttu.edu.vn.